ADVANCED NUMERICAL METHOD FOR ESTIMATE FIRE RESISTANCE OF PARTIALLY ENCASED BEAMS

Piloto, P.A.G. [1]*; Gavilán, Ana Ramos* [2]*; Mesquita, L.M.R.* [1]*.*
[1] *Dep. of Mechanics, Polytechnic Institute of Bragança, Campus Santa Apolónia, ap. 1134, 5301-857 Bragança, Portugal.*
[2] *Dep. of Mechanics, University of Salamanca, Avda. Cardenal Cisneros, 34, 49022 Zamora, Spain.*

ABSTRACT

The ultimate design goal for fire safety engineering is the conception of safe structures. To achieve this goal, advanced calculation methods may be used for the assessment of safety in structures and in particular of structural elements. In order to ensure that ultimate limit requirements are fulfilled, it is necessary to predict failure of each type of material and element during the design process of buildings.
This paper deals with the numerical modelling of partially encased beams, which are composed structural elements, widely used in tall buildings, with two or more different materials and types of construction. Normally are used with reinforcement rebars and with or without structural link to slabs that may use concrete to increase fire resistance.
Instability problems may occur because concrete may not have the age to resist and also because the concrete may slip over steel, crack or crush. Lateral torsional buckling (TLB) is an instability phenomenon that should be considered.
This paper presents Ansys material and geometric non-linear finite element model for determining lateral torsional buckling resistance of partially encased beam with and without encasement reinforcement in fire conditions. The steel part of the composed section will be modelled by finite shell element, concrete part by three-dimensional finite solid elements, the bond slip contact with finite non-linear spring elements and the rebar reinforcement will be considered in perfect contact with concrete, using finite bar element.
Elevated temperatures will be applied in both four sides of the cross section along the beam length, based on ISO834 standard fire. Beams will also be subjected to uniform bending corresponding to a specific degree of load bearing capacity. Failure of concrete will be predicted and based on smeared band approach through modification of the stress - strain fields. Fire resistance will be determined for the last time increment in which it is possible to sustain the equilibrium.

1 INTRODUCTION

Steel beams with partial encasement represent a composite section with two or more different materials, with distinct mechanical behaviour, being usually used in construction for increasing fire resistance, see figure 1.

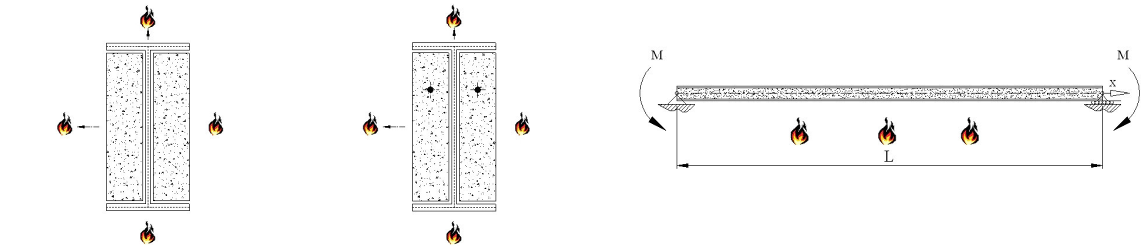

a) Section model without rebars. *b) Section model with rebars.* *b) Beam load model.*

Fig. 1 – Partially encased steel beam with concrete.

Concrete slabs may not transmit the stabilizing effect to prevent lateral torsional buckling (LTB) of partially encased beams. Also, concreting the steel beam within 7 or 8 days provides less torsional stiffness than after 28 days [1]. This instability phenomenon is responsible for a simultaneous lateral displacement and cross-section rotation. This means that bending around the minor axis and torsion about the longitudinal axis of the element are involved.

Experimental tests conducted at room temperature were presented by the Technical University of Berlin [2] and other experimental and numerical results were presented during the European research project for technical steel research, at CTICM and LABEIN [3]. This work intends to be the preliminary phase of a full scale test program in fire conditions, complemented with numerical research and intends to deal with the interaction between concrete and steel, finding failure of concrete that may occur during instability and finding optimal design reinforcement.

Fire resistance for lateral unrestrained partially encased beams, IPE200 with and without reinforced concrete will be determined. Transient non-linear thermal analysis will be subsequently followed by a non linear static analysis to address the ultimate limit state. Partially encased beams will be subjected uniform bending moment equivalent to 50% of the plastic resistant moment value considered without rebars.

2 LATERAL TORSIONAL BUCKLING

Accidental fire conditions reduce the load bearing capacity and increase the risk of failure by lateral instability. The partial concrete protection may not be sufficient to provide stabilizing effect during the increase of steel temperature. Ultimate LTB resistance must be checked in the design phase in order to get the assurance that structures are appropriately safe and resistant regarding the accidental loading conditions.

2.1 Critical Moment

The ideal behaviour of a perfectly straight simply supported beam with perfectly elastic material behaviour, subjected to bending about major axis and prone to LTB is characterized with elastic critical moment (M_{cr}). This value corresponds to the load level at equilibrium bifurcation [3].

For LTB, the critical moment may be determined assuming the validity of the elastic theory (energy method) and some assumptions regarding the concrete strength contribution. Torsion constant and the moment of inertia may be calculated for the composed section based on the characteristic values of steel part and based on the reduced characteristic values of concrete part, as represented in the next expressions [2].

$$J = J_a + J_{c,red}$$
$$I_z = I_{za} + I_{zc,red} \tag{1}$$

J and I_z represent the torsion constant and the moment of inertia of the composed section, $J_{c,red}$ and $I_{zc,red}$ represent the reduced torsion constant and the reduced moment of inertia of concrete, while J_a and I_{za} represent the torsion constant and the moment of inertia of steel. The concrete part is accounted for by reducing this part to an equivalent steel part, $J_{c,red}$ and $I_{zc,red}$, using (2).

$$I_{zc,red} = I_{zc} E_c / E_a$$
$$J_{c,red} = J_c G_c / G_a \tag{2}$$

Taking into consideration only the compressive part of concrete, see figure 2, both geometric properties may be determined according to the notation for the plastic compressive zone, defined by e_{pl}, without the rebars contribution, where f_{ya} and β_R represent the design strength of steel and concrete.

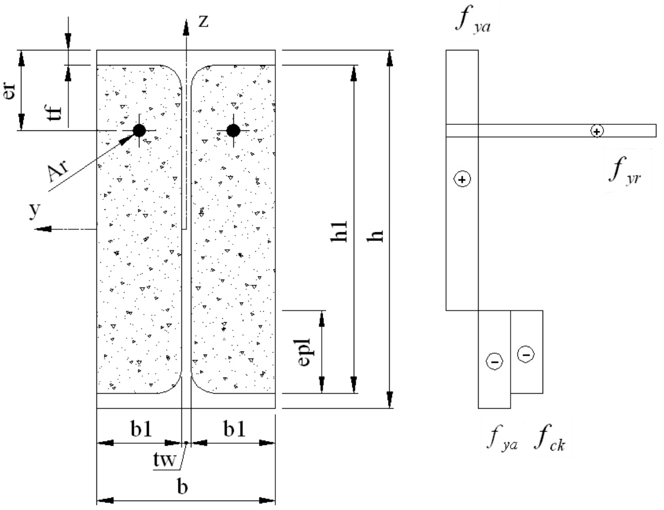

Fig. 2 – Notation for plastic section.

$$e_{pl} = \frac{2 f_{ya}\, t_w\, h_1/2}{2 f_{ya}\, t_w + 2 b_1 \beta_R} \tag{3}$$

The geometric properties of concrete section may de determined according to the previous expression, using the next assumptions.

$$\alpha = \left[1 - 0.63\, e_{pl} / (b - t_w)\right] / 3$$
$$J_c = (b - t_w) e_{pl}^{\,3} \alpha \qquad (4)$$
$$I_{z,c} = e_{pl} (b - t_w)^3 / 12$$

The assumptions of a constant stiffness value along the beam length, considering the influence of the warping restrain small, the influence of moments of inertia much smaller than the influence of torsion constant, may be used to calculate the critical moment. The warping constant of the concrete part is neglected and a symmetric section may be considered [2].
The flexural and torsional stiffness is determined in accordance to the previous equations. Critical moment may be determined taking into account the loading conditions, the moment distribution and the lateral restraints. For uniform bending moment, simple supported beam and double symmetric cross section the critical moment is defined by equation (5).

$$M_{cr} = \frac{\pi}{L} \sqrt{(EI_z)\left(GJ + \frac{\pi^2 EI_w}{L^2}\right)} \qquad (5)$$

2.2 Plastic Moment

Full plastic moment expression is well known for the case of steel beams. For partially encased beams only the plastic compression zone of concrete will be considered, in accordance to the represented model to determine plastic moment with or without rebar reinforcement [2].

$$M_{pl} = M_{pl,a} - \frac{2 f_{ya} t_w (0.5 h_1 - e_{pl})^2}{2} + \beta_R 2 b_1 e_{pl} (0.5 e_{pl} + 0.5 h_1 - e_{pl}) + A_r (f_{yr} - \beta_R)(h - 2 e_r) \qquad (6)$$

$M_{pl,a}$ represents the full plastic moment for the steel section, while A_r and e_r accounts for the reinforcement area and its vertical position. Two reinforcing steel rebars with equivalent diameter to 12 [mm] will be considered. The yield strength of the reinforcing material is considered equal to $f_{yr} = 500\,[MPa]$, at room temperature.

3 THERMAL ANALYSIS

Partially encased beam will be subjected to fire conditions, according to the standard fire nominal curve, ISO 834. Convective heat flux will be applied to the composite member, depending on the bulk temperature and constant convective coefficient $\alpha_c = 25\,[W/m^2K]$. Radiative heat flux will depend on the assumed configuration factor, resultant emissivity, $\varepsilon_{res} = 0.7$, considered for both exposed steel and concrete surfaces, and on the radiation temperature, considered equal to the bulk nominal temperature [4].

The procedure for determining the temperature development for this type of composite members may be based on advanced calculation models. Non linear transient analysis will be used, based on a full finite element incremental time procedure. All heat flux exchanges, between concrete and steel, will consider perfect contact. The reinforcement thermal effect will be responsible for reducing temperature over coincident concrete nodes.

3.1 Numerical Model

Three-dimensional model based on ANSYS shell131, solid70, combine39 and link33 finite elements were used to simulate thermal behaviour of partially encased steel beams with or without reinforced concrete (RC) in fire conditions, see figure 3.

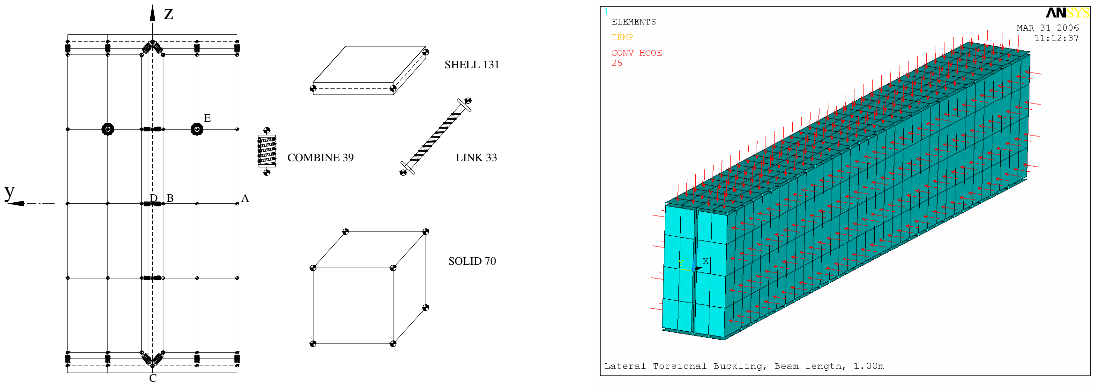

a) Finite elements used to model the beam. b) Finite element mesh.

Fig. 3 – Partially encased beam with reinforced concrete.

Finite shell element (shell131) is a three-dimensional layered shell with four nodes having in-plane and thru-thickness thermal conduction capability. The conducting shell element is applicable to three dimensional transient thermal analyses. Shell131 generates temperatures that can be passed to structural shell elements in order to model the thermo – mechanical behaviour. The shape functions are linear for in-plane interpolation with 2x2 integration scheme, while for thickness (assuming no temperature variation) the shape functions are assumed constant with 1 integration point.

Finite solid element (solid70) has a three-dimensional thermal conduction capability. This element has eight nodes with a single degree of freedom (temperature at each node). The element is used to model concrete three dimensional transient thermal analyses and may be replaced by an equivalent structural element to model thermo-mechanical behaviour. The shape functions are linear in each orthogonal direction and possess a 2x2x2 integration scheme.

Finite combine element (combine39) is a unidirectional finite element defined by two nodes with nonlinear generalized temperature variation – heat flux capability. The element behaviour is defined by the generic curve temperature versus heat flux. The element has no mass or thermal capacitance. The full contact area of steel and concrete was modelled by this non linear spring element, connecting node to node, between steel finite shell element and concrete finite solid element. The bond thermal model considers perfect contact, allowing for all thermal flux to pass throughout the interface in both directions. The heat flux –

temperature variation curve is defined constant and does not input any thermal resistance across interface.

Finite rebar element (link33) is a uniaxial element with the ability to conduct heat between its nodes. The element has a single degree of freedom, temperature, at each node. The conducting bar is applicable to transient thermal analysis. Bar element may be replaced by an equivalent structural element. Shape functions are linear with an exact integration.

3.2 Material Behaviour

Non-linear unsteady state analysis requires the knowledge of steel conductivity and specific heat properties variation with temperature. According to EC3 - part 1.2 [5], for carbon steel (profile and rebars), these properties vary with temperature, as represented in figure 4. Specific mass is assumed to be constant and equal to 8750 [kg/m^3].

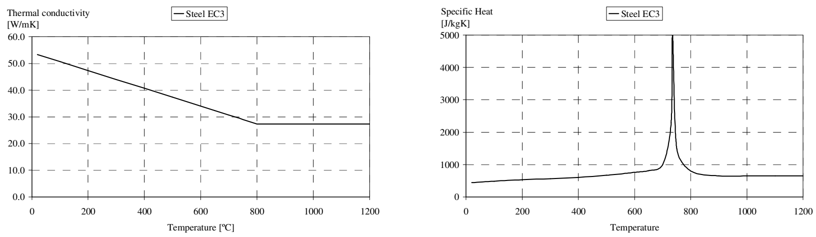

a) Thermal conductivity b) Specific heat.

Fig. 4 – Thermal properties for carbon steel S235 and for reinforcing steel.

Thermal conductivity of concrete, λ_c, may be obtained from Eurocode 2 [6], between lower and upper limit values. The lower limit of thermal conductivity for normal weight concrete was adopted.

Specific heat, $C_p(\theta)$ of dry concrete (u = 0%), depends on temperature and was obtained from the siliceous aggregates [6], according to figure 5.

The variation of the specific mass of concrete with temperature is influenced by water loss during the heating process and is defined as follows [6].

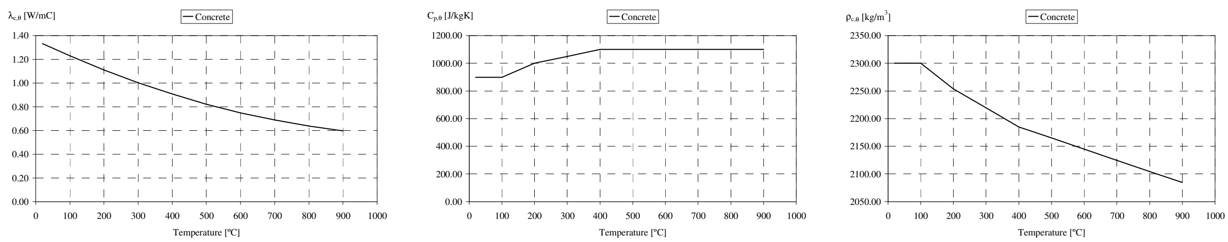

a) Thermal conductivity. b) Specific heat c) Specific mass

Fig. 5 – Thermal properties for concrete C20-25.

3.3 Numerical Results

Numerical results may be presented in time domain. Figure 6 represents the temperature variation across partially encased section. The steel web receives heat, mainly, from both steel beam flanges and less from the adjacent encased concrete.

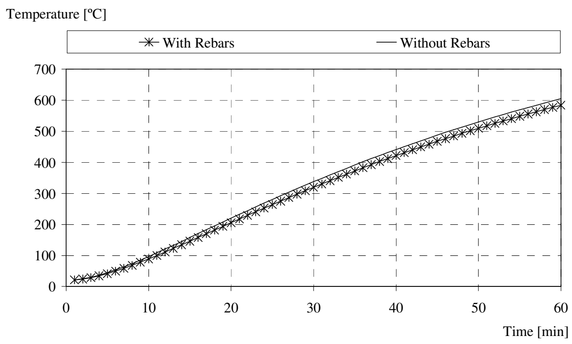

a) Temperature evolution for point E with and without reinforcement (referred to figure 3).

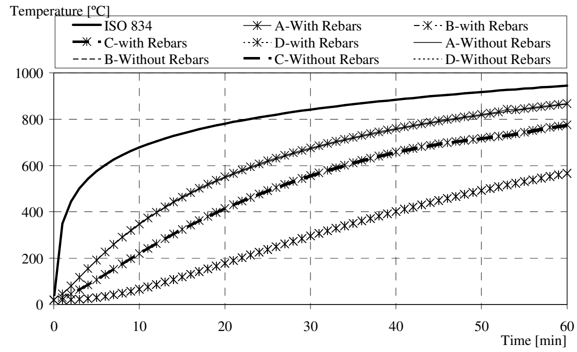

b) Temperature evolution for points A, B, C and D with and without reinforcement (referred to figure 3).

Fig. 6 – Finite element thermal results.

The thermal effect around represented points A,B,C and D is relatively small to produce stiffness modification at that specific locations, see figure 6-b. The presence of reinforcing steel will contribute to decrease concrete temperature around its position, as represented in figure 6-a.

4 THERMO-MECHANICAL ANALYSIS

Partially encased beam will be loaded with 50 % of the design plastic moment, without considering the contribution of reinforcing steel and simultaneously subjected to the increasing temperature obtained in the thermal analysis. Non linear static analysis was undertaken to address the ultimate limit state of instability.

4.1 Numerical Model

Three-dimensional model based on ANSYS shell181, solid65, combine39 and Link 8 finite elements was used to simulate thermo-mechanical behaviour of partially encased steel beams with and without reinforced concrete in fire conditions, see figure 7.

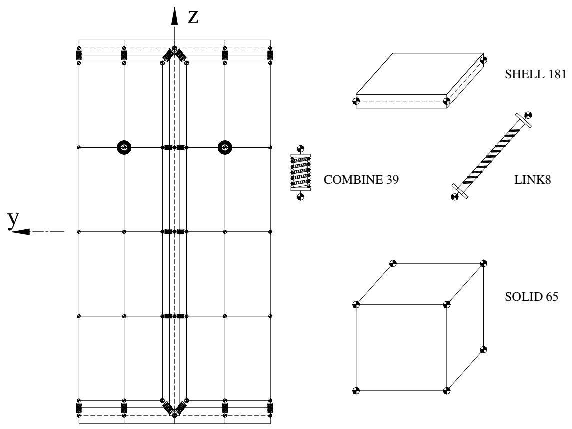

a) Finite elements used to model cross section.

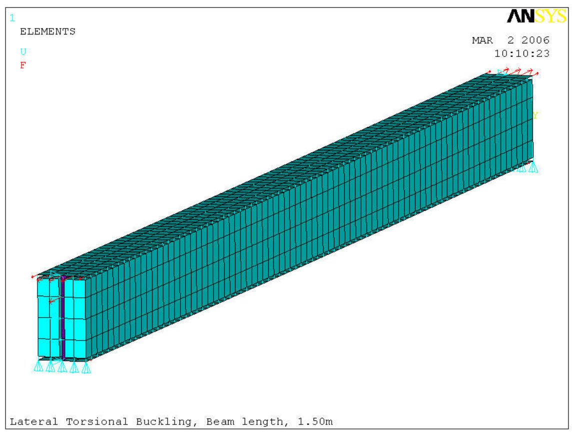

b) Finite element shape representation.

Fig. 7 – Cross section and mesh representation for the thermo-mechanical model.

Finite shell element is suitable for analyzing thin to moderately-thick shell structures. It is a 4-node element with six degrees of freedom at each node: translations in the x, y, and z directions, and rotations about the same axis. This element is also well-suited for material and geometric non-nonlinear applications. Bilinear elements, when fully integrated (2x2, in plane), are too stiff for in-plane bending, nevertheless, full integration scheme was adopted because this element uses the method of incompatible modes to enhance the accuracy in bending-dominated problems [7]. This element is associated with linear elastic and elasto-plastic material properties, being the von Mises isotropic hardening plasticity model used with multilinear isotropic hardening.
Finite solid element is used to model concrete and is capable of cracking in tension and crushing in compression. The element is defined by eight nodes having three degrees of freedom at each node: translations in the nodal x, y, and z directions. This element presents linear shape functions with an integration scheme of 2x2x2.
LINK8 is a spar finite element which may be used to model rebar reinforcement. The 3-D spar element is a uniaxial tension-compression element with three degrees of freedom at each node: translations in the nodal x, y, and z directions. Plasticity and large deflection capabilities are included. Shape functions are linear with an exact integration.
The non linear spring is a uniaxial element defined by two nodes with nonlinear generalized force-deflection capability with large displacement. Figure 8 represents the behaviour of the bond model between concrete and steel, representing the force versus relative displacement. The longitudinal option is a uniaxial tension-compression element with up to three degrees of freedom at each node: translations in the nodal x, y, and z directions. No bending or torsion is considered. The full contact area of steel and concrete was modelled by this non linear spring element, connecting node to node finite shell element and finite solid element. The bond mechanical model was considered equal to the behaviour of the push out tests obtained for concrete –filled steel tubes [8]. When the last data point force is exceeded, the previous slope is maintained.

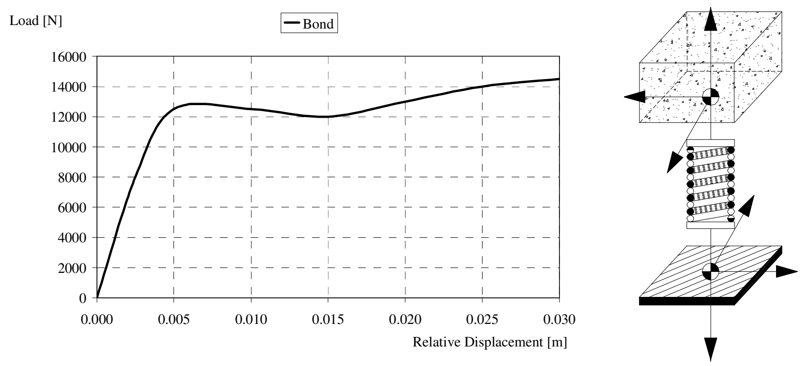

Fig. 8 – Bond interface behaviour between concrete and steel.

The assumption of this bond model ensures that once the peak level force is reached, concrete will travel along the steel with practically no increase in force (curve almost parallel to horizontal axis). This approach may be questionable due to the fact that bond behaviour may

be considered different in tension compared to the compression zones of the flexural member. The element behaviour follows the represented curve in tension and in compression.
Structural elements always present initial imperfections due to fabrication processes, transportation, storage and construction methods. The initial out-of-straightness imperfection causes a secondary bending moment as soon as any compression load is applied, which in turn leads to further bending deflection and a growth in the amplitude of this bending moment. Stable deflected shape equilibrium can be established until the internal compression forces do not exceed the internal moment resistance. The numerical model was implemented with an initial out-of-straightness represented by a harmonic function with $L/400$ of maximum amplitude, to account for global imperfections.
A constant mechanical bending moment is initially applied and thermal load resulting from fire conditions is applied for each time step.

4.2 Material Behaviour

Steel stress-strain relation is based on an elastic- elliptic -plastic model [5], see figure 9. The yield stress at room temperature was considered equal to the characteristic value of steel S235. The elasticity modulus varies with temperature as represented.

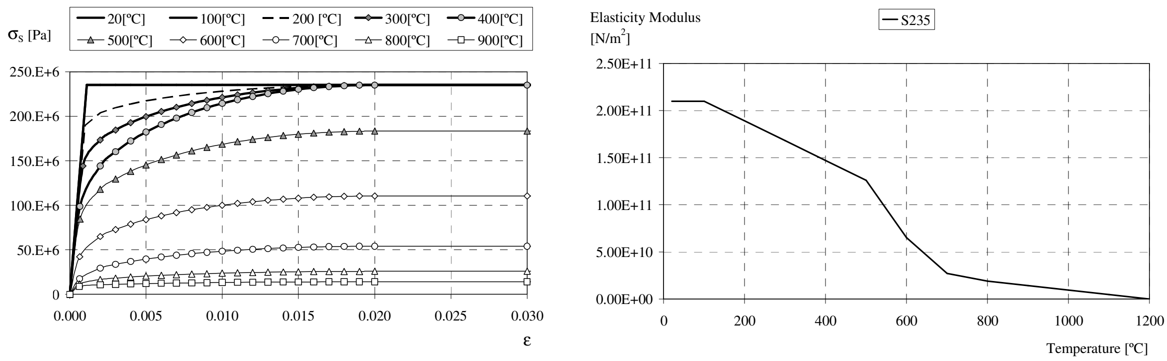

a) Stress – strain versus temperature. b) Elastic modulus versus temperature.

Fig. 9 – Mechanical behaviour of steel S235.

The concrete material is capable of directional integration point cracking and crushing besides incorporating plastic behaviour. Cracking is allowed in three orthogonal directions at each integration point. If cracking occurs at an integration point, the cracking is modelled through an adjustment of material properties which effectively treats the cracking as a “smeared band” of cracks, rather than discrete cracks. In addition to cracking and crushing, the concrete may also undergo plasticity, with William and Warnke failure surface criterion. In this case, the plasticity is verified before the cracking and crushing checks occurs. This material model predicts either elastic behaviour, cracking behaviour or crushing behaviour. If elastic behaviour is predicted, the concrete is treated as a linear elastic material. If cracking or crushing behaviour is predicted, the stress-strain elastic matrix is adjusted for each failure mode. The concrete material is assumed to be initially isotropic.
The presence of a crack failure mode at an integration point is represented through modification of the stress-strain relations by introducing a plane of weakness in a direction

normal to the crack face. If stress relaxing is considered in tension, the secant modulus works with adaptive descent and diminishes to 0.0 as the solution converges, see figure 10. A multiplier coefficient of 1.0 was used for determining the amount of tensile stress relaxation.

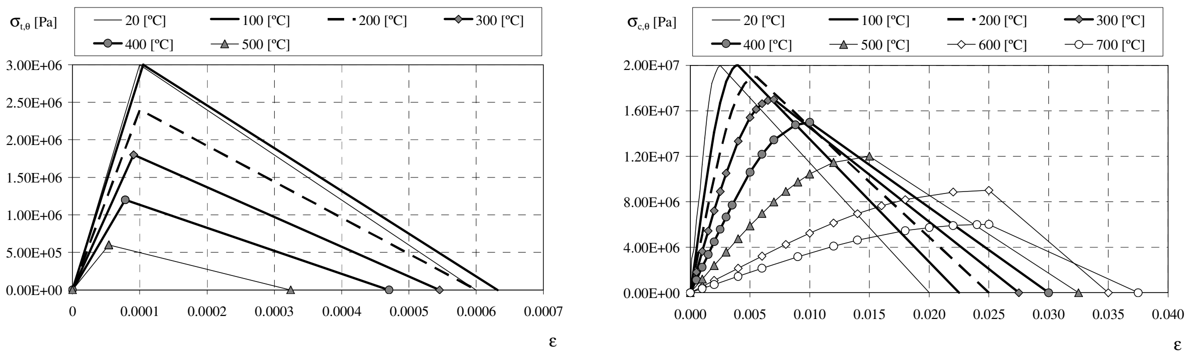

a) Stress-strain behaviour of concrete in tension.

b) Stress-strain behaviour of concrete in compression

Fig. 10 - Strength for concrete material.

The presence of a crushing failure mode at an integration point is defined as the complete deterioration of the material structural integrity. Under these conditions, material strength is assumed to have degraded to an extent such that the contribution to the stiffness of an element at the integration point can be ignored.

The strength and deformation properties of reinforcing steel at elevated temperatures shall be obtained from the stress-strain relationships specified in figure 11.

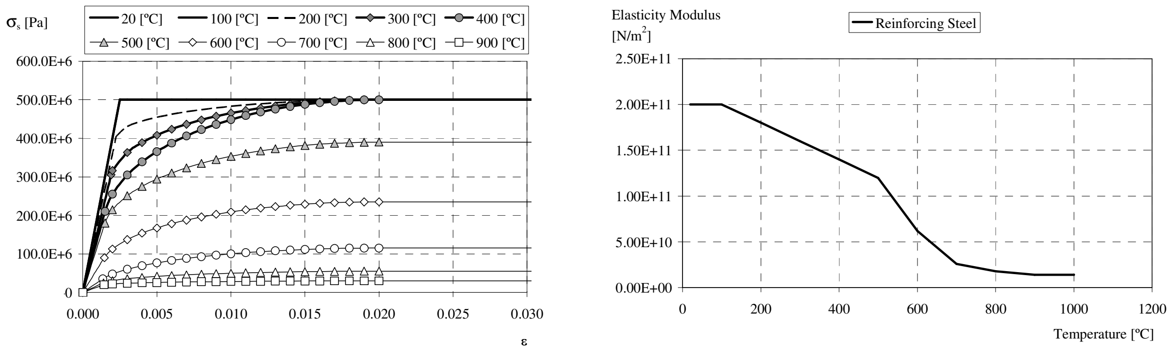

a) Stress – strain versus temperature.

b) Elastic modulus versus temperature.

Fig. 11 –Mechanical behaviour of cold formed reinforcing steel.

The stress-strain relationships given in figure 11 are governed by three parameters, being the slope of the linear elastic range, the proportional limit and the maximum stress level.

4.3 Numerical Results

Fire resistance time will be determined for the last time increment, for which a small temperature increment is responsible for a large displacement and is possible to sustain the equilibrium. As represented in figure 12, concrete cracks after the mechanical load is applied and a progressive failure is verified as the temperature rise.

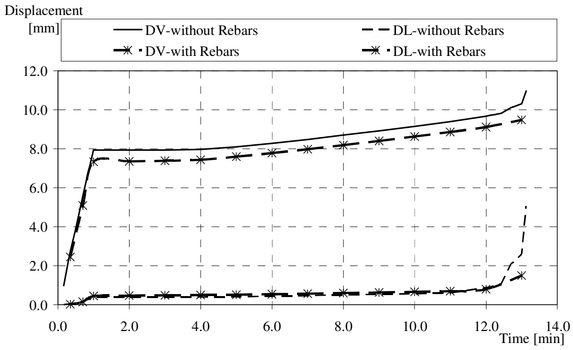

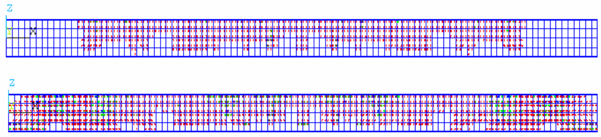

b) Cracking and crushing of concrete at the end of the applied load and at ULS, without concrete reinforcement.

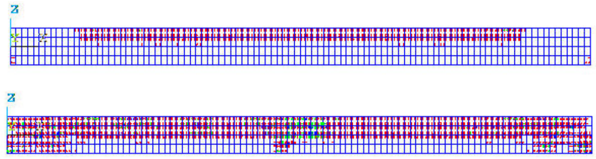

a) Lateral (DL) and vertical (DV) displacements.

c) Cracking and crushing of concrete at the end of the applied load and at ULS, with concrete reinforcement.

Fig. 12 – Results for a beam length of 3 [m], with and without RC.

Cracking and crushing is represented for both cases, with and without reinforced concrete, being this failure mode more developed for the last case. Reinforcement will be responsible for controlling failure, increasing concrete strength contribution for the composed section.

Fire resistance time is represented for different beam slenderness values. Fire resistance decreases as the beam slenderness increase, for the same initial mechanical load.

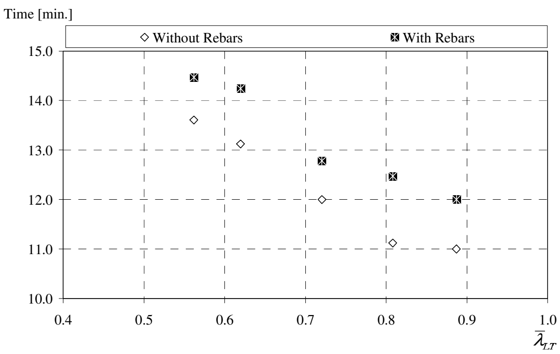

L [m]	$\bar{\lambda}_{LT}$	t [min] without RC	t [min] with RC
2.5	0.56	13.61	14.47
3.0	0.62	13.12	14.24
4.0	0.72	12.00	12.78
5.0	0.81	11.12	12.47
6.0	0.89	11.00	12.00

Fig. 13 – Numerical results of fire resistance time.

5 CONCLUSIONS

A non linear finite element model for determining lateral torsional buckling resistance of partially encased beams in fire conditions was presented. A special attention was considered to the bond model between concrete and steel.

The model predicts the concrete failure by cracking and crushing with and without reinforcing steel.

Fire resistance of partially encased beams subjected to a constant uniform bending moment and to an increasing temperature has been determined.

The results have shown that, for the same mechanical load, as the beams slenderness increases the fire resistance time decreases.

The increase of 10 % average fire resistance results form the steel rebars reinforcing contribution.

REFERENCES

1. Boissonade, N.; Jaspart, J.P.; Maquoi, R.; “Development of a general model for lateral torsional buckling check in the erection phase. Application to partially encased beams, including the restraining effect of metal sheeting”; University of Liège, Department M&S; July 2004.
2. Lindner, Joachim; Budassis, Nikos; “Lateral torsional buckling of partially encased composite beams without concrete slab”; conference proceeding of composite construction in steel and concrete IV, May 28-June 2 of 2000; pp. 117-128, ASCE, 2002.
3. European commission, “Lateral torsional buckling in steel and composite beams”; ISBN 92-894-6414-3; Book 1,2 and 3; Technical steel research final report EUR 20888 EN; August 2002.
4. CEN; EN 1991-2-2; “Eurocode 1, Actions on structures – Part 1-2: General actions - Actions on structures exposed to fire”; November 2002.
5. CEN; EN 1993-1-2; “Eurocode 3, Design of Steel Structures – Part 1-2: General rules, Structural fire design”; April 2005.
6. CEN; EN 1992-1-2, “Eurocode 2: Design of concrete structures - Part 1-2: General rules - Structural fire design”; December 2004.
7. J. C. Simo and F. Armero, "Geometrically nonlinear enhanced strain mixed methods and the method of incompatible modes," IJNME, Vol. 33, pp. 1413-1449, 1992).
8. Brahmachari, Koushik; “Connection and flexural behaviour of steel RHS filled high strength concrete”; Ph.D. thesis presented at the University of Western Sidney, December 1997.